Available online at www.sciencedirect.com

ScienceDirect

European Journal of Radiology Open 2 (2015) 90–100

EUROPEAN JOURNAL OF RADIOLOGY OPEN

www.elsevier.com/locate/ejro

Review

# State-of-the-art imaging of liver fibrosis and cirrhosis: A comprehensive review of current applications and future perspectives

Adrian Huber, Lukas Ebner, Johannes T. Heverhagen, Andreas Christe *

*Department of Radiology, University Hospital of Bern, Inselspital, Freiburgstrasse 10, CH-3010 Bern, Switzerland*

Received 3 April 2015; received in revised form 13 May 2015; accepted 15 May 2015
Available online 26 May 2015

**Abstract**

*Objective:* The purpose of this article is to provide a comprehensive overview of imaging findings in patients with hepatic fibrosis and cirrhosis; and to describe which radiological/clinical modality is best for staging hepatic fibrosis.
*Conclusion:* MR elastography (MRE) appears to be the most reliable method for grading liver fibrosis, although the CT fibrosis score derived from the combination of caudate-to-right-lobe ratio and the diameters of the liver veins significantly correlates with the stage of fibrosis.


*Keywords:* Hepatic fibrosis; Liver cirrhosis; Magnetic resonance elastography (MRE); CT fibrosis score; Fibroscan

## Contents



## 1. Introduction

Hepatic cirrhosis is the pathological sequela of all chronic liver diseases [1]. The most common causes of hepatic cirrhosis are alcoholic fatty liver disease (AFLD), non-alcoholic fatty liver disease (NAFLD) and viral hepatitis [2]. Less frequent causes of cirrhosis are haemochromatosis, alpha1-antitrypsin deficiency, Wilson's disease, biliary cirrhosis and cardiac cirrhosis. Chronic inflammation leads to potentially reversible liver fibrosis and ends in irreversible cirrhosis with the cross-linking of collagen fibres and the formation of regenerative nodules. Pathologists routinely distinguish patterns of predominantly pericentral fibrosis (e.g., in AFLD/NAFLD fibrosis/cirrhosis) [3] from patterns of predominantly periportal fibrosis (e.g., in chronic viral hepatitis, autoimmune hepatitis or biliary disease-induced fibrosis/cirrhosis) [4]. The fibrotic stage is classified according to histological criteria using the METAVIR scoring system whereby stages F1–F4 predominantly assess periportal fibrosis [5] and stages B1–B4 predominantly assess pericentral

* Corresponding author. Tel.: +41 31 632 19 65; fax: +41 31 632 48 74.
*E-mail addresses:* andreas.christe@insel.ch, andreas.christe@hotmail.com (A. Christe).

http://dx.doi.org/10.1016/j.ejro.2015.05.002

fibrosis [6]. Because the two staging systems differ only in the fibrosis pattern (which depends on the aetiology of the fibrosis), the resultant data are comparable in terms of the severity of fibrosis (both stages 1 to 4). A liver with stage 4 fibrosis is equivalent to a cirrhotic liver.

All aetiologies of liver cirrhosis lead to the same process, namely macroscopic parenchymal changes and secondary changes due to portal hypertension. The difference in portal blood supply is thought to be responsible for the atrophy of the left lobe and hypertrophy of the right lobe: the right lobe is fed by the right portal vein which is haemodynamically supplied by the superior mesenteric vein, which drains the upper GI tract and contains higher concentrations of alcohol and toxins than the lower GI tract [7]. The inferior mesenteric vein with blood from the lower GI tract mainly supplies the left portal vein and the left and caudate lobes of the liver. A small cadaver study revealed that the right lobe was more fibrotic than the caudate lobe [8]. The disease process characterised by right lobe atrophy and left lobe hypertrophy is described by the modified caudate-to-right-lobe ratio described by Awaya et al. [9]. Later in the fibrosis/cirrhosis sequence, liver heterogeneity and a nodular surface associated with regeneration processes appear; these changes are more easily detectable radiologically following contrast administration [10–12]. This repair process results not only in the formation of regenerative nodules but also in the compression of the central liver veins. A right liver vein below 7 mm in diameter should raise suspicion for cirrhosis [13]. Indirect changes associated with portal hypertension occur relatively late in the development of cirrhosis and include dilation of the hepatic portal vein to a diameter greater than 14 mm, splenomegaly (>11 cm longitudinal axis distance), porto-systemic collateral vessels (recanalisation of the umbilical vein, gastro-spleno-renal collateral vessels, gastro-oesophageal varices and even rectal varices), ascites and thickening of the bowel walls [14–16]. Routine biochemical and haematological tests are unable to quantify liver fibrosis in approximately 50% of patients [17]. An early diagnosis of liver fibrosis can improve the benefit of early therapeutic interventions prior to the development of irreversible and potentially fatal complications such as loss of liver function, oesophageal variceal bleeding, hepatic encephalopathy and hepatocellular carcinoma [18]. Approximately 80% of all hepatocellular carcinomas (HCC) arise from an underlying cirrhotic liver [19].

## 2. Radiological examinations

### 2.1. Ultrasonography

The accuracy, sensitivity and specificity of regular B-mode sonography for diagnosing liver cirrhosis have been reported to be 64–79%, 52–69% and 74–89%, respectively [20–22]. An irregular or nodular surface and blunt edges or morphological changes in the liver are the most specific signs of cirrhosis on ultrasound (Figs. 1–4). Contrast-enhanced ultrasound with sulphur hexafluoride-filled micro-bubbles covered with a phospholipid shell may more easily detect HCC (+20%) than cirrhosis [23].

Considerable efforts have been devoted to detecting liver cirrhosis noninvasively. An inexpensive and simple approach is sonographic elastography [24], a noninvasive and reliable method of detecting liver cirrhosis. Two techniques for sonographic elastography have been described: transient elastography (Fibroscan) and acoustic radiation force impulse (ARFI) elastography. The area under the receiver operating characteristic (ROC) curve of Fibroscan and ARFI elastography ranges from 0.85 to 0.91 for cirrhosis (fibrosis stage 4) and severe fibrosis (fibrosis stage 3); for moderate fibrosis (fibrosis stages 1 and 2), Fibroscan produces significantly better results than ARFI elastography, with areas under the ROC curve of 0.88 and 0.81, respectively ($p = 0.008$). However, in 2–11% of cases, liver failure is not diagnosed with Fibroscan [25,26]. Another limitation of these techniques is that only a very small volume of the liver can be measured at one time and the accuracy of this measurement is very operator-dependent [27]. The usefulness of these techniques is also limited in obese patients and in patients with ascites, both of which are situations that often occur in patients with hepatic fibrosis [28]. In the case of obese patients, the area under the ROC curve for both Fibroscan and ARFI elastography drops to 0.63.

In conclusion, sonographic elastography is an inexpensive and accurate method of diagnosing hepatic cirrhosis. However, this approach is operator-dependent and of limited usefulness for detecting early pre-cirrhotic stages of liver fibrosis in cases of inhomogeneous fibrosis, in obese patients and in patients with ascites.

### 2.2. Computer-tomography (CT)

Abdominal CT scans are increasingly performed in routine clinical studies in hospitals and radiology institutes. A careful examination of the liver parenchyma and a thorough screening for fibrosis in CT scans is mandatory, particularly for patients with no suspected liver pathology. Numerous characteristic imaging findings associated with liver cirrhosis have been described; however, the diagnostic accuracy of CT scans remains disappointing. Imaging findings suggestive of liver cirrhosis include an irregular or nodular hepatic surface, a blunt liver edge, parenchymal abnormalities, morphological changes in the liver and manifestations of portal hypertension (Figs. 5–8). In a multicentre study conducted by Kudo et al., the diagnostic accuracy, sensitivity and specificity of CT for hepatic cirrhosis were 67–86%, 77–84% and 53–68%, respectively [20,29].

Harbin et al. developed a cirrhosis score for transverse imaging using the ratio of the width of the transverse caudate lobe to the width of the transverse right lobe. The sensitivity, specificity and accuracy of this score for detecting cirrhotic livers were 84%, 100% and 94%, respectively. A relative widening of the porta hepatis was sensitive but not specific for liver cirrhosis [8] (Fig. 5).

Few studies have investigated the accuracy of CT findings in pre-cirrhotic liver fibrosis. Measures such as the modified caudate-to-right-lobe ratio [9] and a decrease in the diameter of the liver vein [13] have been used to detect liver remodelling on MR images. The combination of both of these variables (i.e., the

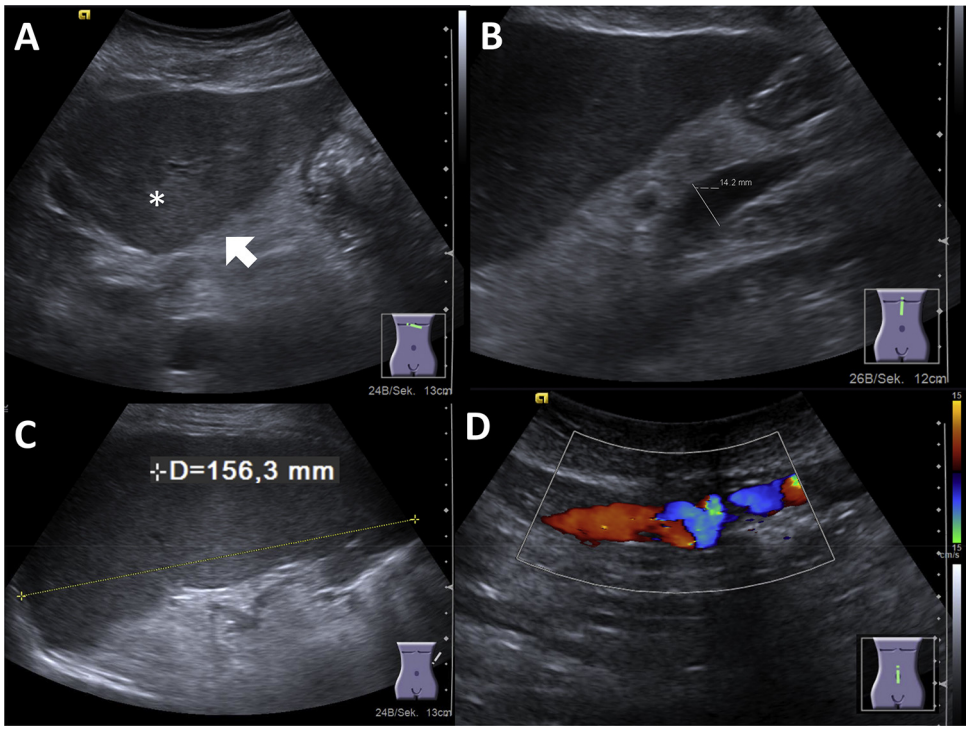


Fig. 1. (A) Liver cirrhosis in ultrasonography: inhomogeneous liver parenchyma (asterisk) with surface nodularity (arrow). (B) Portal venous hypertension with dilation of portal vein, splenomegaly (C) and collateral vessels within the abdominal wall (D).

sum of liver vein diameters divided by the caudate-to-right-lobe ratio) has been used as a CT fibrosis score with a sensitivity of 83% and a specificity of 76% for pre-cirrhotic liver fibrosis [30] (Fig. 6) and a sensitivity of 88% and specificity of 82% for liver cirrhosis. This score represents a new way of diagnosing pre-cirrhotic liver fibrosis and an improvement over the diagnostic ability of CT scans for liver cirrhosis (sensitivity of 77–84% and specificity of 53–68% for CT [20]). Other imaging findings

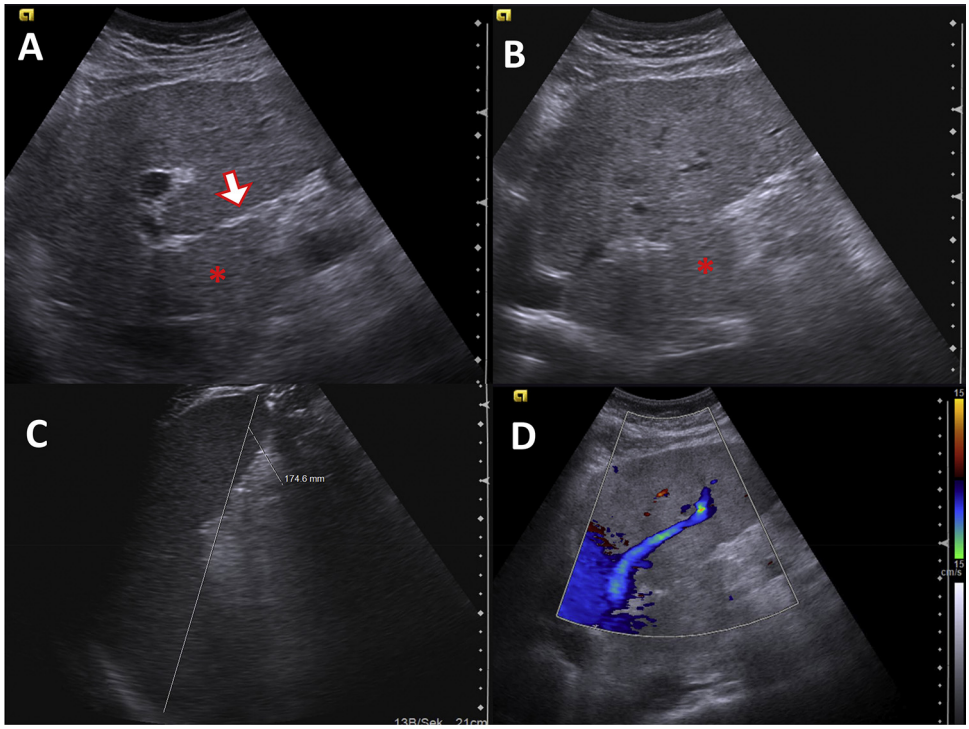


Fig. 2. Ultrasonography of a 25-year-old patient suffering from haemochromatosis. (A) Inhomogenous liver parenchyma with surface nodularity (white arrow). (B) Caudate lobe is enlarged (asterisk, sagittal plane). (C) Splenomegaly 17 cm. (D) Hepatofugal flow in the left portal vein (stream inversion).

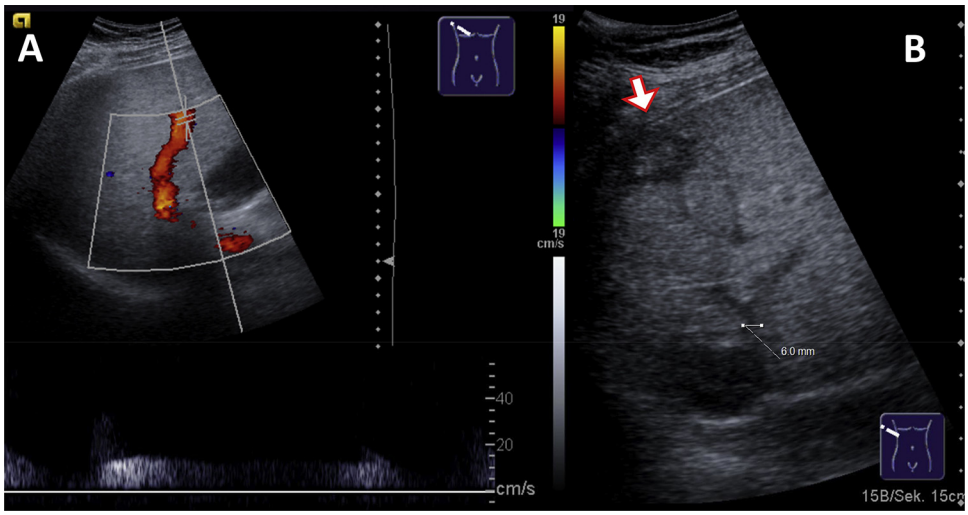


Fig. 3. Ultrasonography of a 64-year-old male patient suffering from Laennec's cirrhosis. (A) Regular hepatopetal blood flow in the right portal vein. (B) Remodelling of the liver with compression of the middle hepatic vein (6 mm diameter), note the HCC in the periphery of the liver (white arrow).

associated with hepatic cirrhosis and their ability to differentiate between normal hepatic fibrosis and cirrhosis are listed in Table 1. The fibrosis score derived from the combination of these two variables was shown to correlate significantly with the grade of fibrosis obtained by CT [30].

CT scans could be used to screen for liver fibrosis and justify the use of more accurate diagnostic methods. In particular, patients with a potentially reversible stage of liver fibrosis could benefit from an early diagnosis and early initiation of therapy.

One limitation of diagnostic CT is the dose of radiation associated with its use. Technical improvements in CT technology, including the use of automated CT tube current modulation, care voltage, new image reconstruction algorithms (iterative reconstruction) and the latest generation of CT detectors in which electronics and the photodiode are combined into a single unit could reduce the dose of radiation used in a diagnostic abdominal scan by more than 50%. Nevertheless, the average equivalent dose of an abdominal scan is approximately 5 mSv (millisievert),

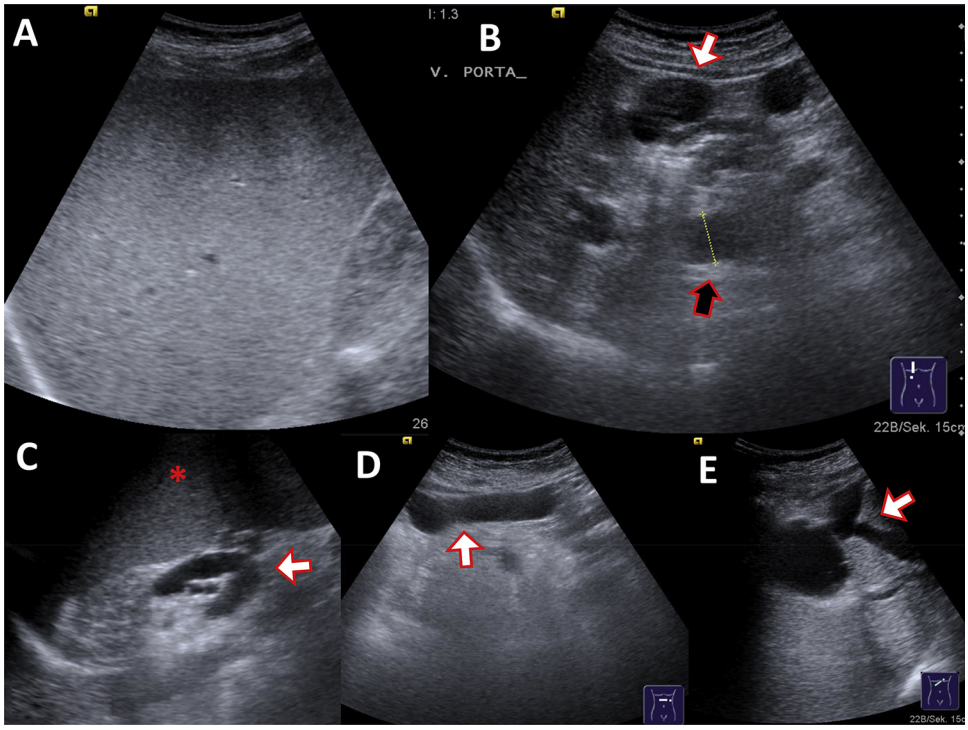


Fig. 4. Ultrasonography of a 64-year-old female patient suffering from hepatitis C induced cirrhosis. (A) Hyperechoic fatty liver. (B) Massive collateral vessels (umbilical vein, white arrow), dilated main portal vein (black arrow, 19 mm). (C) Gastrolienal collateral veins and splenomegaly. (D) Dilated umbilical vein. (E) Subhepatic collateral veins.

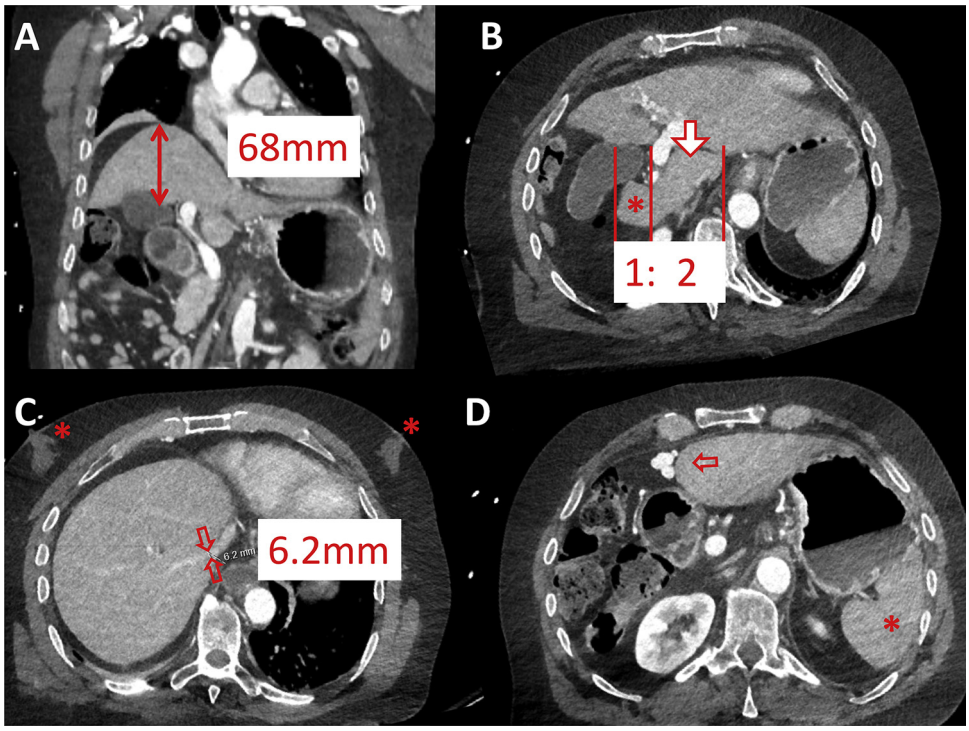


Fig. 5. (A, B) CT of liver cirrhosis with right lobe atrophy and left lobe hypertrophy complex with a caudate (arrow) to right (asterisk) lobe ratio >1. (C) Right vein diameter <7 mm due to compression of cirrhotic liver parenchyma; note additional gynecomasty (asterisk). (D) Signs of portal venous hypertension with recanalisation of umbilical vein and therefore no extensive splenomegaly (asterisk).

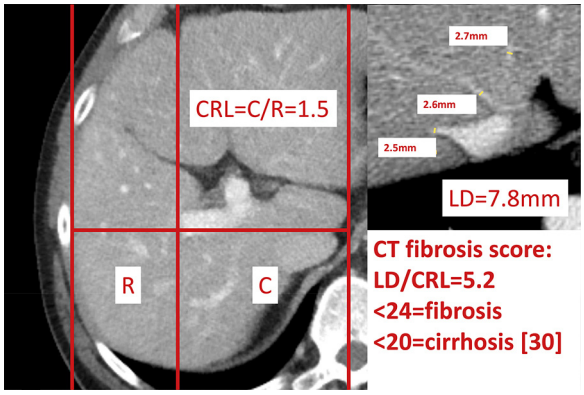


Fig. 6. Pathologic caudate–right-lobe ratio (CRL) in a patient with pre-cirrhotic liver fibrosis (CT): hypertrophy of the left and atrophy of the right liver. In axial planes a line parallel to the midsagittal plane was drawn through the right lateral wall of the first bifurcation of the right portal vein. Distances perpendicular to the drawn line to the most medial margin of the caudate lobe and the lateral margin of the right lobe midway between the main portal vein and the inferior caval vein were measured. The two distances were divided (caudate lobe/right lobe) and defined as the caudate–right-lobe ratio (CRL). The sum of liver vein diameters (LD) equals 7.8 mm. LD divided by CRL equals the CT fibrosis score, which is below 20 and therefore compatible with liver cirrhosis.

which corresponds to a risk of radiation-induced cancer death of 1/5000 per CT scan [31–33].

Until now, the measurement of liver stiffness by CT had not been possible because of the potentially harmful dose of radiation and the availability of the radiation-free alternatives sonography and MR. The advantage of CT imaging lies in its ability to rapidly detect HCC and perform staging following contrast injection [34,35].

### 2.3. Magnetic resonance imaging

Surface nodularity, heterogeneous enhancement, a small liver size, caudate lobe enlargement, splenomegaly, a decreased right-to-left-lobe-volume ratio, varices, an expanded gallbladder fossa [36,37], a posterior notch and ascites [38] are well known features of liver cirrhosis [13] (Figs. 9–12). Nevertheless, the sensitivity and specificity of classic contrast-enhanced MRI for liver cirrhosis are 87% and 54%, respectively, which are similar to the sensitivity and specificity of CT [20]. Awaya et al. observed that the hypertrophied portion of the right lobe of the liver appears to extend beyond the bifurcation of the main portal vein (Harbin's caudate-to-right-lobe ratio) and to the right lateral edge of the ligamentum venosum where the right portal vein bifurcates (modified caudate-to-right-lobe ratio or CRL). In the case of a CRL greater than 0.90, the sensitivity, specificity and accuracy of MR imaging for cirrhosis were 71.7%, 77.4% and 74.2%, respectively. In contrast, the maximum accuracy achieved with Harbins's CRL was 65.7%. Only the modified CRL enabled these authors to find significant differences in the ratios of the three Child–Pugh classes [9]. Zhang et al. were able to increase the sensitivity and specificity for liver cirrhosis to 88% and 85%, respectively, by measuring the diameter of hepatic veins only, as the regenerative nodules and fibrosis associated with cirrhosis tend to compress the hepatic veins; the best cut-off diameter for the right hepatic vein was 7 mm [13].

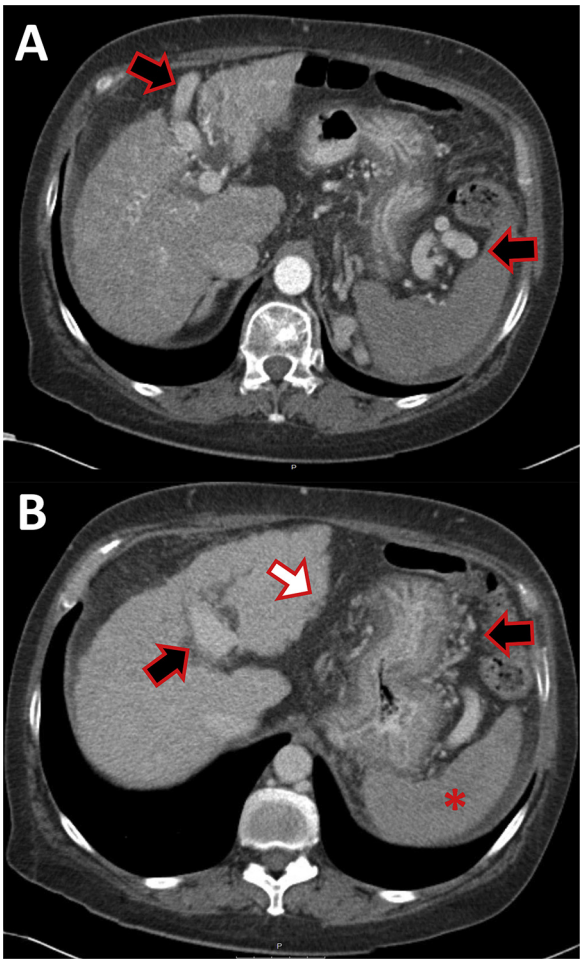


Fig. 7. CT of a 58-year-old female patient with alcoholic liver cirrhosis. Large collateral vessels (black arrows): re-opened umbilical vein (A), gastro-lienal collaterals (B). Because of the re-opening of the umbilical vein the spleen (asterisk) usually does not enlarge. Note the nodularity of the liver surface (white arrow).

MR elastography [39], double contrast-enhanced MRI [40], diffusion-weighted MRI [41], susceptibility-weighted MRI [42,43] and T1rho [44] are able to detect liver fibrosis in a pre-cirrhotic stage with great accuracy. Double-contrast MRI uses superparamagnetic iron oxide (SPIO) particles that accumulate in hepatic Kupffer cells and lead to a shortening of the T2* relaxation time, producing a dark liver background. By comparison, gadolinium-based contrast media leads to a delayed enhancement of the septal and bridging fibrosis [40]. Both contrast agents facilitate the visualisation of early fibrosis and the differentiation of advanced hepatic fibrosis from mild or absent fibrosis with an accuracy of 93% [45].

Fibrotic tissue restricts the diffusion of water molecules. Consequently, diffusion-weighted imaging should depict different stages of fibrosis (Fig. 9); however, inconsistent results for staging liver fibrosis have been reported [17,41,46]. The sensitivity and specificity of diffusion-weighted MRI with single-shot echo-planar technique using a hepatic apparent diffusion coefficient (ADC) at *b* values of 50, 300, 500, 700, and 1000 s/mm$^2$ have been reported to be up to 83% and 89%, respectively, for stage 2 fibrosis or greater [41]. These results may vary because the ADC is dependent on perfusion, hepatic steatosis, hepatic iron stores and hepatic inflammation [40].

Susceptibility-weighted MRI (SWI) is a 2D GRE-based SWI sequence [42] that detects small amounts of paramagnetic material due to their faster relaxation time. This sequence has been used to detect the deposition of paramagnetic iron in cerebral haemorrhages. In a fibrotic liver, small amounts of iron that can be detected by SWI are always present in regenerative nodules. The loss in the paramagnetic signal is proportional to the degree of liver remodelling. The liver-to-muscle signal intensity (SI) ratio is strongly correlated with fibrosis, moderately correlated with inflammatory activity and iron load and not correlated with steatosis. The liver-to-muscle-SI ratio performed well in terms of grading liver fibrosis, with a sensitivity and specificity of 98% and 82%, respectively, for scores of F2 or higher and 80% and 89%, respectively, for a score of F4 (liver cirrhosis) [43].

T1rho is another promising MR technique used to diagnose liver fibrosis. This approach measures the relaxation of motion-restricted water molecules and their local macromolecular environment (e.g., proteoglycan or collagen in the extracellular matrix). T1rho values are prolonged with the accumulation of compounds in the extracellular matrix [47]. Mean liver T1rho values greater than 50 ms using a 2D TurboFLASH sequence with spin-lock preparation are associated with a sensitivity and specificity of 90.5% and 90%, respectively [44].

MR elastography (MRE) appears to be the most reliable of these new MRI-based methods [48]. MRE analyses the propagation of mechanical waves through tissue [49]. The velocity and wavelength of these waves increase with greater tissue stiffness [50]. Thus, images of the propagating waves can be used to estimate tissue stiffness. Motion-sensitising gradients are applied during the acquisition of the image. The gradients are similar to those applied in phase-contrast MR angiography and diffusion-weighted imaging [40]. Patients are placed in the supine position with a pneumatic driver placed over the liver on the anterior abdominal wall. The pneumatic driver generates mechanical waves by vibrating at low frequencies (40–120 Hz). The waves propagating into the liver are measured with a MRI-protocol with 2D gradient-echo sequences and cyclic motion-encoding gradients (MEG). Specialised computer-based algorithms analyse these mechanical waves. Quantitative images measuring shear stiffness (MR elastograms) are generated and liver stiffness is calculated in kPa. Yin et al. showed that MR elastography with a shear stiffness cut off value of 2.93 kPa had a sensitivity of 98% and a specificity of 99% for diagnosing any grade of liver fibrosis (grades 1–4) [51]. MR elastography appears to be highly accurate for detecting fibrosis early and measuring the stiffness of the entire liver. Salameh et al. showed that MR elastography accurately measured liver stiffness in rats with steatohepatitis even before they developed hepatic fibrosis according to histological criteria [52]. MRE could be used to differentiate nonalcoholic fatty liver disease (NAFLD) from nonalcoholic steatohepatitis (NASH) before patients develop liver fibrosis [53]. MR elastography has a sensitivity of 98% and specificity of 99% [51] and is being discussed as an alternative to liver biopsy as the gold standard for diagnosing and monitoring liver fibrosis; indeed, MRE is highly accurate, non-invasive and can measure the entire

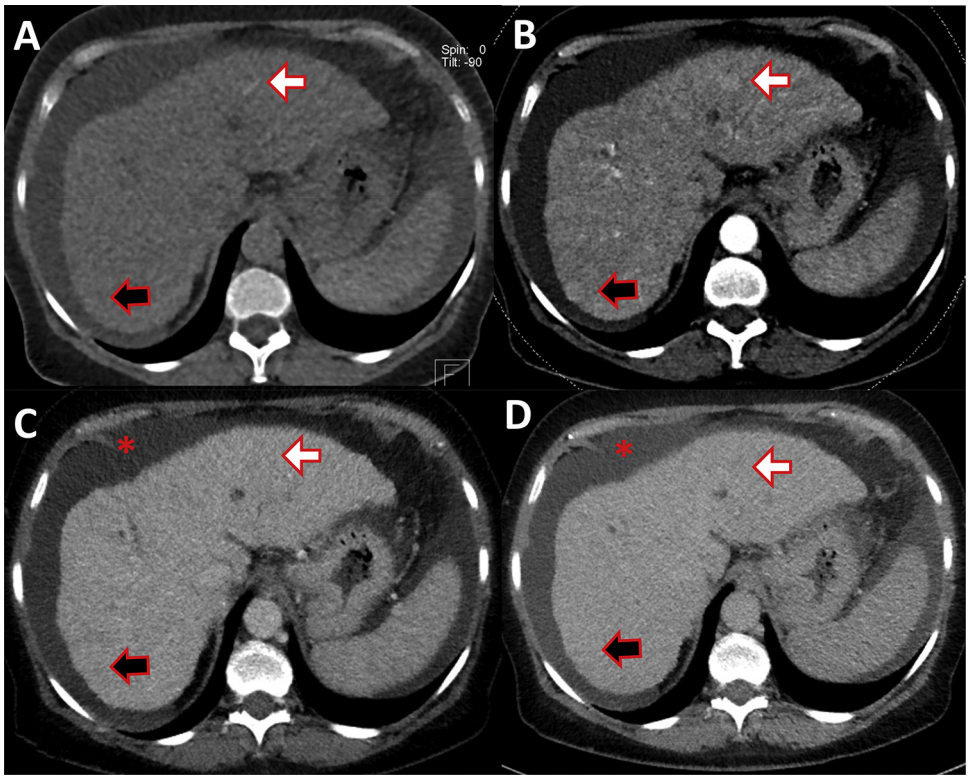


Fig. 8. CT of a 57-year-old female patient, suffering from alcoholic liver cirrhosis. (A) Native phase without contrast. (B) Late arterial phase. (C) Portal venous phase. (D) Equilibrium phase. Atrophic liver with ascites is evident. Early nodular enhancement is depictable in the arterial phase (white arrow, B), there is no wash-out of this liver nodule, compatible with a regenerative or dysplastic nodule, HCC is less probable. Other regenerative nodules with the same enhancement pattern are shown (black arrow). Ascites on all slices is evident (asterisk).

hepatic volume, whereas a liver biopsy only evaluates a small volume of the liver and is dependent on the quality of the biopsy and the experience of the pathologist. Elasticity cutoff values and corresponding areas under the receiver operating characteristic curves have been described for the different stages of liver fibrosis [54]; stages F1–F4 correspond to elasticity cutoff values of 2.84, 3.18, 3.32 and 4.21 kPa, respectively, and areas under the ROC curve of 0.91, 0.92, 0.97 and 0.99, respectively. MR elastography has been shown to have greater sensitivity (at least 4% higher) and much more specificity (at least 15% greater) than DWI for each stage of fibrosis [55].

MR elastography is also preferable to US elastography because an acoustic window is not needed, obese patients can be reliably examined and no observer variability exists. In addition, the entire liver can be assessed with MRE, whereas only small regions of interest can be viewed with US elastography. However, MR elastography is of limited value in patients with hepatitis or cardiac congestion or in patients with increased

Table 1
Area under the receiver operating characteristic (ROC) curve of CT predictors for liver fibrosis and cirrhosis [30].

| | Cirrhotic versus normal liver (signs of cirrhosis) AUC | Fibrotic versus normal liver (signs of fibrosis) AUC | Cirrhotic versus fibrotic liver AUC |
|---|---|---|---|
| Right hepatic vein diameter | 0.86 | 0.74 | 0.64 |
| Middle hepatic vein diameter | 0.82 | 0.71 | 0.62 |
| Left hepatic vein diameter | 0.85 | 0.77 | 0.62 |
| Sum of all hepatic vein diameters (LD) | 0.88 | 0.79 | 0.65 |
| Caudate-to-right lobe ratio (CRL) | 0.82 | 0.72 | 0.66 |
| CT fibrosis score: LD/CRL | **0.89** | **0.82** | 0.69 |
| Splenic diameter | 0.88 | 0.76 | 0.66 |
| Portal diameter | 0.64 | 0.58 | 0.59 |
| Ascites | 0.78 | 0.55 | 0.66 |
| Collateral vessels | 0.86 | 0.58 | **0.73** |
| Liver nodularity | 0.87 | 0.69 | 0.68 |

AUC, area under the curve (receiver operating characteristic analysis).
Best discriminators have bold values.

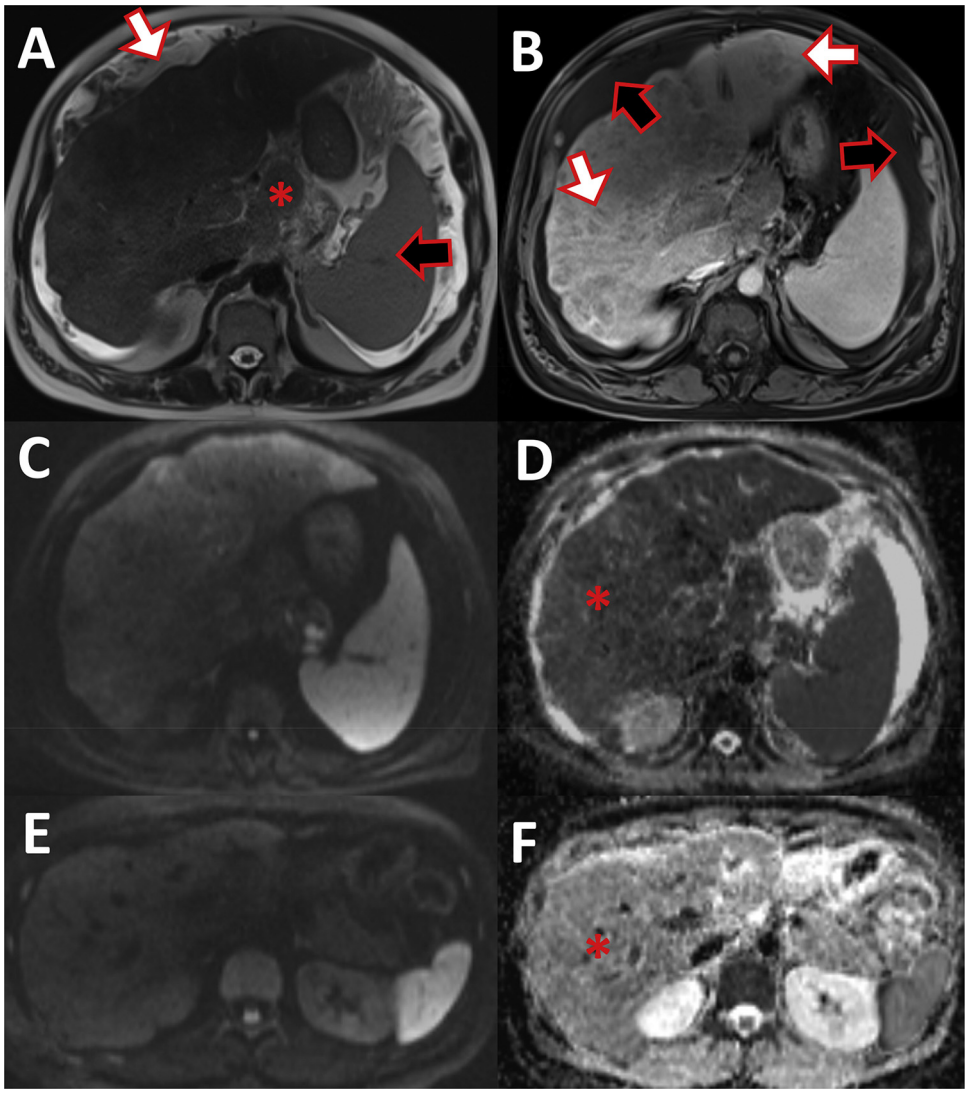


Fig. 9. Liver cirrhosis in MRI. (A) T2 haste sequence: nodular liver surface (white arrow) with hypertrophic caudate lobe (asterisk) and splenomegaly (black arrow). (B) T1 vibe fat saturated post-gadolinium image displays the inhomogeneous liver parenchyma with many hypovascular regenerative nodules (white arrow) and ascites (black arrow). (C) Diffusion weighted image b800 showed slight inhomogeneous intensity of the liver. (D) Ep2d diffusion ADC-maps displays hypointense liver signal (asterisk) compared to a normal liver MRI. (E) Diffusion weighted image b800 of a normal liver with homogeneous liver signal. (F) Ep2d diffusion ADC-maps of normal liver with brighter signal than the cirrhotic liver (D).

hepatic iron stores, as these conditions introduce signal-to-noise limitations, making wave visualisation impossible [27,49,51].

### 2.4. High-resolution multifrequency MRE

Multifrequency MRE is preferable for detecting liver fibrosis because monofrequency MRE produces standing waves with non-undulating wave nodes that do not permit elastographic measurement. As a result, the special resolution is very low and only the stiffness of the entire liver can be measured. This limitation can be overcome with multifrequency MRE; this technique enables the definition of a high-resolution map of liver stiffness, delivering exact 3D data and allowing the analysis of focal fibrosis and the evaluation of focal liver lesions [56].

MRE has been successfully used to diagnose diastolic dysfunction by identifying abnormalities in myocardial relaxation [57]. Elasticity scores of healthy kidneys and spleens that could be used to detect focal fibrotic disease have recently been published [56]. Neurodegenerative processes could also be diagnosed using MRE imaging of the brain in patients with multiple sclerosis [58].

### 2.5. Laboratory

CT scans can be used to screen for liver fibrosis and justify the use of more accurate diagnostic methods such as first-line serologic testing and the well-established and easily performed Fibroscan. The most important laboratory tests of liver function are serum aspartate aminotransferase, alkaline phosphatase, alanine aminotransferase and γ-glutamyl transpeptidase activity. The activity of all of these parameters has been shown to be significantly altered in cases of mild, moderate and severe fibrosis ($p = 0.01–0.05$); however, in a multiple regression analysis including the aforementioned parameters and SWI, only SWI

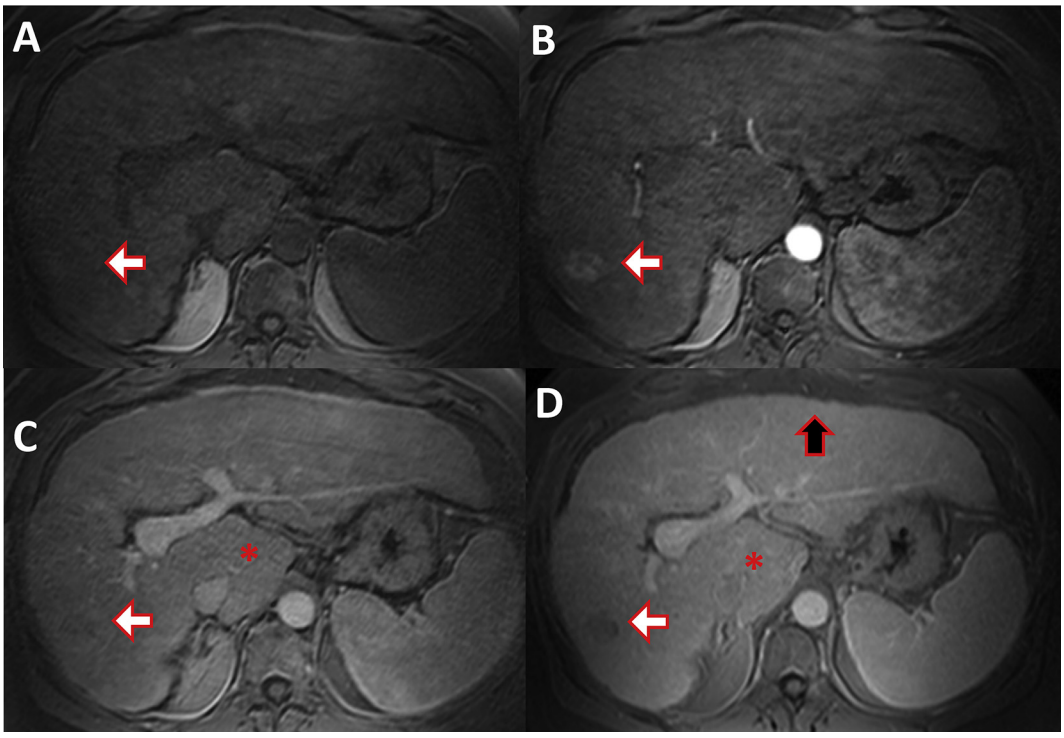


Fig. 10. MRI of a 61-year-old male patient with hepatitis B induced liver cirrhosis and HCC. (A) T1 weighted fat saturated native phase without contrast. (B) Late arterial phase. (C) Portal venous phase. (D) Equilibrium phase. Early HCC enhancement is demonstrated in the arterial phase (white arrow, B), there is wash-out of the contrast media in the later phases (C, D). Surface nodularity (black arrow) and hypertrophy of the caudate lobe (asterisk) with atrophy of the right liver is evident.

proved to be independently associated with increasing fibrosis scores [43]. Degos et al. [59] showed that Fibroscan could more reliably detect the stage of fibrosis in patients with chronic viral hepatitis than a biomarker (Hepascore, APRI, Fibrotest®, and Fibrometre®).

### 2.6. Biopsy

A liver biopsy is currently the gold standard for diagnosing liver cirrhosis. However, it entails an invasive procedure and often produces biased results because very small specimens are taken (only 1/50,000th of the liver is analysed) and because sampling errors and inter-rater variability can occur [27]. The limited number of locations where the biopsy can be performed and the associated risks of infection and haemorrhage are the main disadvantages of an invasive biopsy. Biopsies have morbidity and mortality rates of 3% and 0.03%, respectively [60].

According to the American Association for the Study of Liver Diseases, only patients with substantial liver fibrosis (F2 and

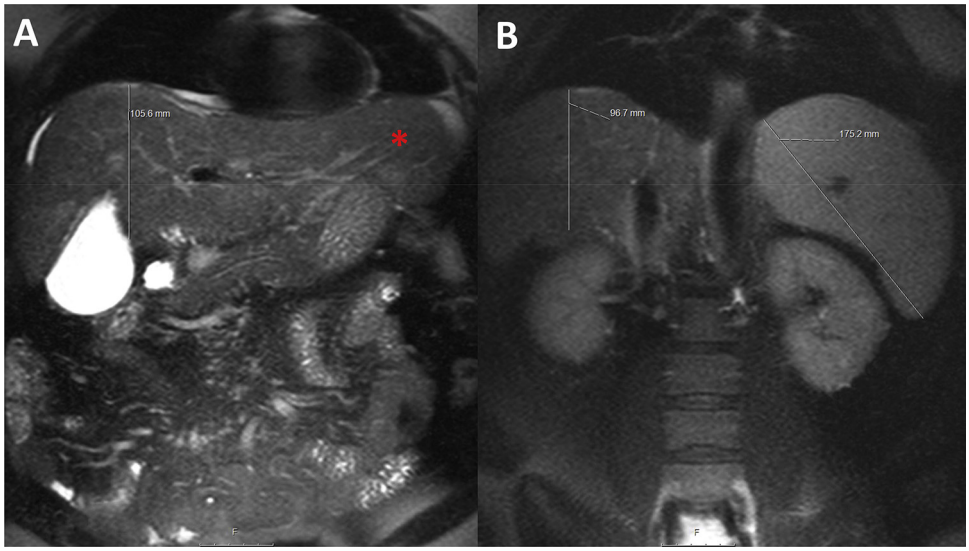


Fig. 11. MRI of a 48-year-old female patient suffering from hepatitis B and C. Coronal T2 haste fat saturated images at the level of the gall bladder (A) and the kidneys (B). Small atrophic right liver with a cranio-caudal distance of 10 cm and prominent left liver (asterisk) with splenomegaly (17.5 cm).

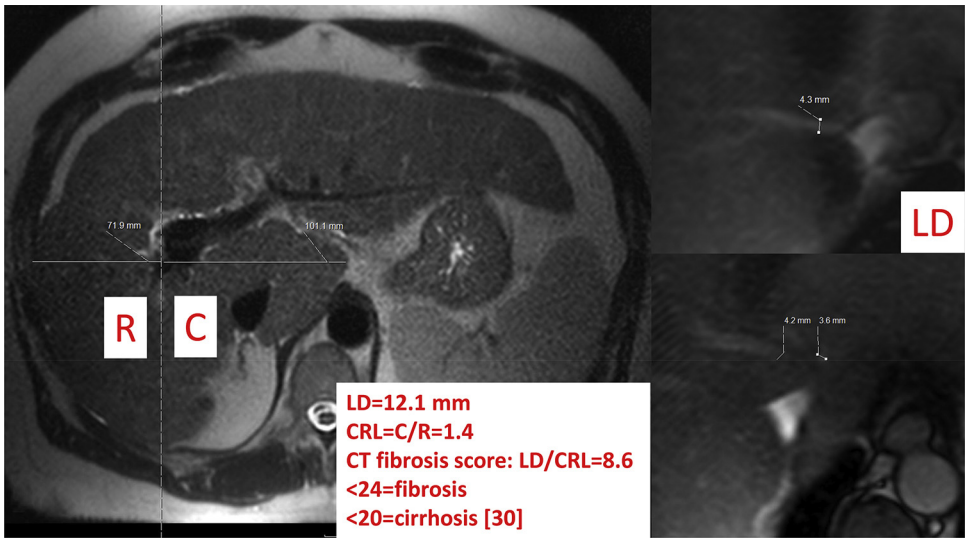


Fig. 12. Pathologic caudate–right-lobe ratio (CRL) in a patient with hepatitis B induced liver cirrhosis (MRI, T2 weighted haste): hypertrophy of the left and atrophy of the right liver. A dashed line parallel to the midsagittal plane was drawn through the right lateral wall of the first bifurcation of the right portal vein. The two distances of the caudate lobe (C) and right lobe (R) were divided and defined as the caudate–right-lobe ratio (CRL). The sum of the three liver vein diameters (LD) equals 12.1 mm. LD divided by CRL equals the CT fibrosis score, which is below 20 and therefore compatible with liver cirrhosis.

greater) are eligible for antiviral therapy; therefore, establishing the exact grade of fibrosis is essential.

## 3. Conclusion

Liver fibrosis and cirrhosis are increasingly common in patient populations with a growing incidence of obesity, physical inactivity and alcohol consumption. Patients with known risk factors, abnormal clinical and laboratory liver findings or altered imaging results can be screened for liver fibrosis. A reduced hepatic vein diameter and an elevated caudate-to-right-lobe ratio are important early imaging findings indicative of liver fibrosis. A CT fibrosis score, which combines these two variables, has been shown to be the most accurate measure for predicting cirrhosis.

The simplest and least expensive approach to evaluate a suspected liver fibrosis is sonographic elastography using either transient elastography (Fibroscan) or acoustic radiation force impulse (ARFI) elastography.

Advanced imaging methods using magnetic resonance imaging such as MR elastography have been shown to be superior to sonographic elastography in the early stages of suspected liver fibrosis and in patients who have medical conditions that preclude the use of sonographic elastography (e.g., obese patients).

Other advantages of MR imaging techniques are their ability to assess the entire liver and the lack of inter-rater variability that affects sonographic elastography or liver biopsies; for this reason, MR elastography could replace liver biopsy as a new diagnostic gold standard.

## Conflict of interest

The authors and author's institutions have no conflicts of interest.

## References

[1] Poynard T, Mathurin P, Lai CL, Guyader D, Poupon R, Tainturier MH, et al. A comparison of fibrosis progression in chronic liver diseases. J Hepatol 2003;38(3):257–65.
[2] Schuppan D, Afdhal NH. Liver cirrhosis. Lancet 2008;371(9615):838–51.
[3] Friedman SL. Seminars in medicine of the Beth Israel Hospital, Boston. The cellular basis of hepatic fibrosis. Mechanisms and treatment strategies. N Engl J Med 1993;328(25):1828–35.
[4] Ishak KG. Pathologic features of chronic hepatitis: a review and update. Am J Clin Pathol 2000;113(1):40–55.
[5] Bedossa P, Poynard T. An algorithm for the grading of activity in chronic hepatitis C. The METAVIR Cooperative Study Group. Hepatology 1996;24(2):289–93.
[6] Brunt EM, Janney CG, Di Bisceglie AM, Neuschwander-Tetri BA, Bacon BR. Nonalcoholic steatohepatitis: a proposal for grading and staging the histological lesions. Am J Gastroenterol 1999;94(9):2467–74.
[7] Mizumoto R, Kawarada Y, Suzuki H. Surgical treatment of hilar carcinoma of the bile duct. Surg Gynecol Obstet 1986;162:153–8.
[8] Harbin WP, Robert NJ, Ferrucci Jr JT. Diagnosis of cirrhosis based on regional changes in hepatic morphology: a radiological and pathological analysis. Radiology 1980;135(2):273–83.
[9] Awaya H, Mitchell DG, Kamishima T, Holland G, Ito K, Matsumoto T. Cirrhosis: modified caudate–right lobe ratio. Radiology 2002;224(3):769–74.
[10] Dodd 3rd GD, Baron RL, Oliver 3rd JH, Federle MP. Spectrum of imaging findings of the liver in end-stage cirrhosis: part I. Gross morphology and diffuse abnormalities. Am J Roentgenol 1999;173(4):1031–6.
[11] Brancatelli G, Federle MP, Ambrosini R, Lagalla R, Carriero A, Midiri M, et al. Cirrhosis: CT and MR imaging evaluation. Eur J Radiol 2007;61(1):57–66.
[12] Ito K, Mitchell DG, Kim MJ, Awaya H, Koike S, Matsunaga N. Right posterior hepatic notch sign: a simple diagnostic MR finding of cirrhosis. J Magn Reson Imaging 2003;18(5):561–6.
[13] Zhang Y, Zhang XM, Prowda JC, Zhang HL, Sant'anna Henry C, Shih G, et al. Changes in hepatic venous morphology with cirrhosis on MRI. J Magn Reson Imaging 2009;29(5):1085–92.
[14] Brown JJ, Naylor MJ, Yagan N. Imaging of hepatic cirrhosis. Radiology 1997;202(1):1–16.
[15] Gupta D, Chawla YK, Dhiman RK, Suri S, Dilawari JB. Clinical significance of patent paraumbilical vein in patients with liver cirrhosis. Dig Dis Sci 2000;45(9):1861–4.

[16] Karahan OI, Dodd 3rd GD, Chintapalli KN, Rhim H, Chopra S. Gastrointestinal wall thickening in patients with cirrhosis: frequency and patterns at contrast-enhanced CT. Radiology 2000;215(1):103–7.
[17] Lewin M, Poujol-Robert A, Boëlle PY, Wendum D, Lasnier E, Viallon M, et al. Diffusion-weighted magnetic resonance imaging for the assessment of fibrosis in chronic hepatitis C. Hepatology 2007;46(3):658–65.
[18] Garcia-Tsao G. Current management of the complications of cirrhosis and portal hypertension: variceal hemorrhage, ascites, and spontaneous bacterial peritonitis. Gastroenterology 2001;120(3):726–48.
[19] Gentilini P, Laffi G, La Villa G, Romanelli RG, Buzzelli G, Casini-Raggi V, et al. Long course and prognostic factors of virus-induced cirrhosis of the liver. Am J Gastroenterol 1997;92(1):66–72.
[20] Kudo M, Zheng RQ, Kim SR, Okabe Y, Osaki Y, Iijima H, et al. Diagnostic accuracy of imaging for liver cirrhosis compared to histologically proven liver cirrhosis. Intervirology 2008;51(Suppl. 1):17–26.
[21] Cardi M, Muttillo IA, Amadori L, Petroni R, Mingazzini P, Barillari P, et al. Superiority of laparoscopy compared to ultrasonography in diagnosis of widespread liver diseases. Dig Dis Sci 1997;42:546–8.
[22] DiLelio A, Cestari C, Lomazzi A, Beretta L. Cirrhosis: diagnosis with sonographic study of the liver surface. Radiology 1989;172:389–92.
[23] Chen LD, Xu H, Xie X, Xie XH, Xu ZF, Liu GJ, et al. Intrahepatic cholangiocarcinoma and hepatocellular carcinoma: differential diagnosis with contrast-enhanced ultrasound. Eur Radiol 2010;20(3):743–53.
[24] Sandrin L, Fourquet B, Hasquenoph JM, Yon S, Fournier C, Mal F, et al. Transient elastography: a new noninvasive method for assessment of hepatic fibrosis. Ultrasound Med Biol 2003;29(12):1705–13.
[25] Cassinotto C, Lapuyade B, Aït-Ali A, Vergniol J, Gaye D, Foucher J, et al. Liver fibrosis: noninvasive assessment with acoustic radiation force impulse elastography – comparison with FibroScan M and XL probes and FibroTest in patients with chronic liver disease. Radiology 2013;269(1):283–92.
[26] Pang JX, Pradhan F, Zimmer S, Niu S, Crotty P, Tracey J, et al. The feasibility and reliability of transient elastography using Fibroscan®: a practice audit of 2335 examinations. Can J Gastroenterol Hepatol 2014;28(3):143–9.
[27] Schmeltzer PA, Talwalkar JA. Noninvasive tools to assess hepatic fibrosis: ready for prime time? Gastroenterol Clin N Am 2011;40(3):507–21.
[28] Glaser KJ, Manduca A, Ehman RL. Review of MR elastography applications and recent developments. J Magn Reson Imaging 2012;36(4):757–74.
[29] Honda H, Onitsuka H, Masuda K, Nishitani H, Nakata H, Watanabe K. Chronic liver disease: value of volumetry of liver and spleen with computed tomography. Radiat Med 1990;8:222–6.
[30] Huber A, Ebner L, Montani M, Semmo N, Heverhagen J, Christe A. CT findings in liver fibrosis and cirrhosis. Swiss Med Wkl 2014;144:w13923.
[31] Huda W, Magill D, He WCT. Effective dose per dose length product using ICRP 103 weighting factors. Med Phys 2011;38(3):1261–5.
[32] Ning P, Zhu S, Shi D, Guo Y, Sun M. X-ray dose reduction in abdominal computed tomography using advanced iterative reconstruction algorithms. PLOS ONE 2014;9(3):e92568.
[33] Risk estimations for radiation protection. NCRP report 115; 1993.
[34] Hennedige T, Venkatesh SK. Imaging of hepatocellular carcinoma: diagnosis, staging and treatment monitoring. Cancer Imaging 2013;12(3):530–47.
[35] Kudo M, Izumi N, Kokudo N, Matsui O, Sakamoto M, Nakashima O, et al. Management of hepatocellular carcinoma in Japan: Consensus-Based Clinical Practice Guidelines proposed by the Japan Society of Hepatology (JSH) 2010 updated version. Dig Dis 2011;29(3):339–64.
[36] Ito K, Mitchell DG, Gabata T, Hussain SM. Expanded gallbladder fossa: simple MR imaging sign of cirrhosis. Radiology 1999;211:723–6.
[37] Verma SK, Mitchell DG, Bergin D, Lakhman Y, Austin A, Verma M, et al. Dilated cisternae chyli: a sign of uncompensated cirrhosis at MR imaging. Abdom Imaging 2009;34(2):211–6.
[38] Gualdi GF, Volpe A, Polettini E, Ceroni AM, Pirolli FM, Casciani E. The role of magnetic resonance in the evaluation of diffuse liver diseases. Clin Ther 1994;144:539–44.
[39] Rustogi R, Horowitz J, Harmath C, Wang Y, Chalian H, Ganger DR, et al. Accuracy of MR elastography and anatomic MR imaging features in the diagnosis of severe hepatic fibrosis and cirrhosis. J Magn Reson Imaging 2012;35(6):1356–64.
[40] Faria SC, Ganesan K, Mwangi I, Shiehmorteza M, Viamonte B, Mazhar S, et al. MR imaging of liver fibrosis: current state of the art. Radiographics 2009;29(6):1615–35.
[41] Taouli B, Tolia AJ, Losada M, Babb JS, Chan ES, Bannan MA, et al. Diffusion-weighted MRI for quantification of liver fibrosis: preliminary experience. Am J Roentgenol 2007;189(4):799–806.
[42] Dai Y, Zeng M, Li R, Rao S, Chen C, DelProposto Z, et al. Improving detection of siderotic nodules in cirrhotic liver with a multi-breath-hold susceptibility weighted imaging technique. J Magn Reson Imaging 2011;34(2):318–25.
[43] Balassy C, Feier D, Peck-Radosavljevic M, Wrba F, Witoszynskyj S, Kiefer B, et al. Susceptibility-weighted MR imaging in the grading of liver fibrosis: a feasibility study. Radiology 2014;270(1):149–58.
[44] Rauscher I, Eiber M, Ganter C, Martirosian P, Safi W, Umgelter A, et al. Evaluation of T1ρ as a potential MR biomarker for liver cirrhosis: comparison of healthy control subjects and patients with liver cirrhosis. Eur J Radiol 2014;83(6):900–4.
[45] Aguirre DA, Behling CA, Alpert E, Hassanein TI, Sirlin CB. Liver fibrosis: noninvasive diagnosis with double contrast material-enhanced MR imaging. Radiology 2006;239(2):425–37.
[46] Boulanger Y, Amara M, Lepanto L, Beaudoin G, Nguyen BN, Allaire G, et al. Diffusion-weighted MR imaging of the liver of hepatitis C patients. NMR Biomed 2003;16(3):132–6.
[47] Wang YX, Yuan J, Chu ES, Go MY, Huang H, Ahuja AT, et al. T1rho MR imaging is sensitive to evaluate liver fibrosis: an experimental study in a rat biliary duct ligation model. Radiology 2011;259:712–9.
[48] Wang QB, Zhu H, Liu HL, Zhang B. Performance of magnetic resonance elastography and diffusion-weighted imaging for the staging of hepatic fibrosis: a meta-analysis. Hepatology 2012;56(1):239–47.
[49] Manduca A, Oliphant TE, Dresner MA, Mahowald JL, Kruse SA, Amromin E, et al. Magnetic resonance elastography: non-invasive mapping of tissue elasticity. Med Image Anal 2001;5(4):237–54.
[50] Talwalkar JA, Yin M, Fidler JL, Sanderson SO, Kamath PS, Ehman RL. Magnetic resonance imaging of hepatic fibrosis: emerging clinical applications. Hepatology 2008;47(1):332–42.
[51] Yin M, Talwalkar JA, Glaser KJ, Manduca A, Grimm RC, Rossman PJ, et al. A preliminary assessment of hepatic fibrosis with magnetic resonance elastography. Clin Gastroenterol Hepatol 2007;5(10):1207–13.
[52] Salameh N, Larrat B, Abarca-Quinones J, Pallu S, Dorvillius M, Leclercq I, et al. Early detection of steatohepatitis in fatty rat liver by using MR elastography. Radiology 2009;253(1):90–7.
[53] Chen J, Talwalkar JA, Yin M, Glaser KJ, Sanderson SO, Ehman RL. Early detection of nonalcoholic steatohepatitis in patients with nonalcoholic fatty liver disease by using MR elastography. Radiology 2011;259(3):749–56.
[54] Asbach P, Klatt D, Schlosser B, Biermer M, Muche M, Rieger A, et al. Viscoelasticity-based staging of hepatic fibrosis with multifrequency MR elastography. Radiology 2010;257(1):80–6.
[55] Wang Y, Ganger DR, Levitsky J, Sternick LA, McCarthy RJ, Chen ZE, et al. Assessment of chronic hepatitis and fibrosis: comparison of MR elastography and diffusion-weighted imaging. Am J Roentgenol 2011;196(3):553–61.
[56] Guo J, Hirsch S, Streitberger KJ, Kamphues C, Asbach P, Braun J, et al. Patient-activated three-dimensional multifrequency magnetic resonance elastography for high-resolution mechanical imaging of the liver and spleen. Rofo 2014;186(3):260–6.
[57] Elgeti T, Knebel F, Hättasch R, Hamm B, Braun J, Sack I. Shear-wave amplitudes measured with cardiac MR elastography for diagnosis of diastolic dysfunction. Radiology 2014;271(3):681–7.
[58] Streitberger KJ, Sack I, Krefting D, Pfuller C, Braun J, Paul F, et al. Brain viscoelasticity alteration in chronic-progressive multiple sclerosis. PLoS ONE 2012;7:e29888.
[59] Degos F, Perez P, Roche B, Mahmoudi A, Asselineau J, Voitot H, et al. Diagnostic accuracy of FibroScan and comparison to liver fibrosis biomarkers in chronic viral hepatitis: a multicenter prospective study (the FIBROSTIC study). J Hepatol 2010;53(6):1013–21.
[60] Janes CH, Lindor KD. Outcome of patients hospitalized for complications after outpatient liver biopsy. Ann Intern Med 1993;118(2):96–8.